Proc. Natl. Acad. Sci. USA
Vol. 96, pp. 9727–9732, August 1999
Genetics

Expression pattern of the mouse ortholog of the Pendred's syndrome gene (*Pds*) suggests a key role for pendrin in the inner ear

LORRAINE A. EVERETT*, HAKIM MORSLI†, DORIS K. WU†, AND ERIC D. GREEN*‡

*Genome Technology Branch, National Human Genome Research Institute, National Institutes of Health, Bethesda, MD 20892; and †National Institute on Deafness and Other Communication Disorders, National Institutes of Health, Rockville, MD 20850

Communicated by Maynard V. Olson, University of Washington, Seattle, WA, June 16, 1999 (received for review March 30, 1999)

ABSTRACT **Pendred's syndrome is an autosomal-recessive disorder characterized by deafness and goiter. After our recent identification of the human gene mutated in Pendred's syndrome (*PDS*), we sought to investigate in greater detail the expression of the gene and the function of its encoded protein (pendrin). Toward that end, we isolated the corresponding mouse ortholog (*Pds*) and performed RNA *in situ* hybridization on mouse inner ears (from 8 days postcoitum to postnatal day 5) to establish the expression pattern of *Pds* in the developing auditory and vestibular systems. *Pds* expression was detected throughout the endolymphatic duct and sac, in distinct areas of the utricle and saccule, and in the external sulcus region within the cochlea. This highly discrete expression pattern is unlike that of any other known gene and involves several regions thought to be important for endolymphatic fluid resorption in the inner ear, consistent with the putative functioning of pendrin as an anion transporter. These studies provide key first steps toward defining the precise role of pendrin in inner ear development and elucidating the pathogenic mechanism for the deafness seen in Pendred's syndrome.**

Pendred's syndrome [Online Mendelian Inheritance in Man (OMIM) no. 274600; see http://www3.ncbi.nlm.nih.gov/Omim] is a relatively common, autosomal-recessive disorder characterized by deafness and goiter (1–3). The goiter is variable in its severity but typically presents around puberty (2, 4). Patients usually have a positive perchlorate discharge test (2, 3), whereby an increased amount of unincorporated iodide is released from the thyroid after perchlorate challenge. The latter indicates that the defect in Pendred's syndrome relates to the organification of iodide, either in iodide transport into the follicular lumen or in its binding to thyroglobulin.

The deafness in Pendred's syndrome is typically congenital, profound, and sensorineural in nature, although its presentation is variable and can be of later onset. Patients typically have structural malformations of the inner ear, most classically a Mondini malformation (5–7), where the cochlea is missing its apical turn and has an underdeveloped modiolus (the central bony portion of the cochlea). This cochlear malformation is often associated with several other characteristic defects, including enlargement of the vestibular aqueducts. It is also becoming increasingly apparent that many Pendred's syndrome patients have enlarged vestibular aqueducts as the only radiological defect (8–10), without the classical Mondini malformation. All of these defects are suggestive of a developmental arrest at 7 weeks of human embryonic development. In addition, it has been noted that patients with Mondini malformations usually have reduced numbers of hair cells and spiral ganglion cells (11); these latter microscopic defects are thought to lead to the deafness.

We recently identified the Pendred's syndrome gene (*PDS*) by use of a positional cloning strategy (12). Numerous Pendred's syndrome-associated mutations have now been identified (9, 10, 13–16). The encoded protein, named pendrin, is closely related to numerous known proteins from a large taxonomic span, including plants, yeast, and bacteria. Whereas most of these proteins are sulfate transporters, recent evidence indicates that pendrin does not effectively transport sulfate; rather, it appears to function as an iodide/chloride transporter (17). These important findings, coupled with the known organification defect in Pendred's syndrome, suggest that pendrin may function in the thyroid to transport iodide into the follicular lumen before its incorporation into thyroglobulin. In contrast to this emerging model for pendrin function in the thyroid, its role in the inner ear remains more obscure.

Recognizing that detailed studies of *PDS* expression and pendrin function in the inner ear would best be performed in a nonhuman mammalian system, we have pursued the characterization of the mouse ortholog (*Pds*). Here we report the isolation and sequencing of mouse *Pds* and the examination of its expression in the developing mouse inner ear.

MATERIALS AND METHODS

cDNA Isolation and Sequencing. Mouse poly(A)$^+$ kidney cDNA was either prepared from poly(A)$^+$ RNA (CLONTECH) by using the Advantage RT for PCR kit (CLONTECH) or obtained as ready-prepared poly(A)$^+$ cDNA (Multiple Choice cDNAs, Origene Technologies Rockville, MD). PCR was performed by using the Advantage cDNA polymerase mixture (CLONTECH) according to conditions recommended by the manufacturer. 5′- and 3′-rapid amplification of cDNA ends was performed as above but with Marathon-Ready cDNA (CLONTECH). Often, the resulting products were sequenced directly (as opposed to being cloned first). To derive sequence near the 5′-end of the cDNA, it was sometimes necessary to design sequencing primers with portions complementary to two adjacent exons (thereby avoiding the concurrent sequencing of products amplified from contaminating genomic DNA). The resulting sequence data was managed and assembled with the LASERGENE Seqman II module from DNAstar (Madison, WI). Primers for both PCR and sequencing were designed by using MACVECTOR 6.5 (Oxford Molecular Oxford). Primer sequences are available on request.

The publication costs of this article were defrayed in part by page charge payment. This article must therefore be hereby marked "*advertisement*" in accordance with 18 U.S.C. §1734 solely to indicate this fact.

PNAS is available online at www.pnas.org.

Abbreviations: dpc, days postcoitum; P, postnatal day.

Data deposition: The sequences reported in this paper have been deposited in the GenBank database (accession nos. AF167411 and AF167412).

‡To whom reprint requests should be addressed at: Genome Technology Branch, National Human Genome Research Institute, National Institutes of Health, 49 Convent Drive, Building 49, Room 2A08, Bethesda, MD 20892. E-mail: egreen@nhgri.nih.gov.

After amplification, PCR products were purified on a Microcon-100 column (Amicon) or treated with exonuclease I (Amersham Pharmacia) and shrimp alkaline phosphatase (Amersham Pharmacia) at 37°C for 30 minutes followed by heat inactivation at 80°C for 15 minutes. Sequencing reactions were performed by using ABI Prism BigDye terminators [Perkin–Elmer/Applied Biosystems; diluted 1:3 or 1:7 with a solution of 80 mM Tris·HCl (pH 9.0) and 2 mM $MgCl_2$], ≈20 ng/kilobase DNA, and 6 pmol of sequencing primer. The cycle-sequencing conditions consisted of 93°C for 3 minutes followed by 25 cycles of 94°C for 30 seconds, 55°C for 5 seconds, and 60°C for 3.5 minutes. Samples were then purified on 96-well gel filtration blocks (Edge Biosystems, Gaithersburg, MD) or Centrisep columns (Princeton Separations, Adelphia, NJ) and analyzed on a model 377 sequencing instrument (Perkin–Elmer/Applied Biosystems).

RNA *in Situ* Hybridization. A ≈1.7-kilobase fragment of *Pds* was amplified from mouse kidney cDNA (prepared as described above) by using primers containing 5′ tails with *Xho*I and *Spe*I restriction sites, respectively (5′TACGAT*CTCGAG*-CAAAAACTACAACGGCATCCTCTC3′ and 5′TAC-GAT*ACTAGT*GCTGCTGAAGTGCAAAGAAACAG3′). The resulting PCR product was digested with *Xho*I and *Spe*I, ligated into *Xho*I–*Spe*I-digested pBluescript II (Stratagene), and transformed into DH5α cells (Life Technologies, Rockville, MD). The authenticity of the selected clone was verified by sequencing. Riboprobes were derived from the above clone and used for *in situ* hybridization of fetal and P5 mouse inner ear sections. Embryos were staged according to Theiler (18). Whole-mount *in situ* hybridization studies were performed on mouse embryos ranging from 8–10.5 dpc (days postcoitum) (19). Embryos older than 11.5 dpc were processed for cryostat sectioning (19). RNA probes for *Bmp4* (bone morphogenetic protein-4) and *Tyrp2* (tyrosinase-related protein-2) were prepared as described (19, 20).

RESULTS

Isolation of Mouse *Pds*. To isolate and characterize the mouse *Pds* cDNA, low-stringency PCR was performed with human *PDS*-specific primers and mouse kidney poly(A)$^+$ cDNA. The sequence derived from the resulting PCR products was then used to design mouse *Pds*-specific primers, which in turn were used to amplify and sequence the intervening cDNA segments. This iterative process was coupled with 5′- and 3′-rapid amplification of cDNA ends (21), eventually yielding the complete sequence of the ≈3-kilobase mouse *Pds* cDNA (GenBank accession no. AF167411). The mouse *Pds* transcript is considerably shorter than the ≈5-kilobase human *PDS* cDNA because of a shorter 3′-untranslated region (524 bp vs. 2,359 bp). The coding regions of the human and mouse genes share 85% nucleotide identity. The predicted pendrin amino acid sequences are 87% identical (Fig. 1). In contrast, the 3′-untranslated regions of the human and mouse genes are much less related. As an aside, a similar approach was used to isolate and sequence the rat *Pds* cDNA (GenBank accession no. AF167412), in this case using mouse *Pds*-specific primers for performing low-stringency PCR. The rat *Pds* sequence is 85% and 93% identical to its human and mouse orthologs, respectively. The predicted rat pendrin amino acid sequence is 88% and 96% identical to human and mouse pendrin, respectively (Fig. 1).

***Pds* Expression in the Mouse Inner Ear.** A key rationale for isolating the mouse *Pds* gene was to facilitate expression

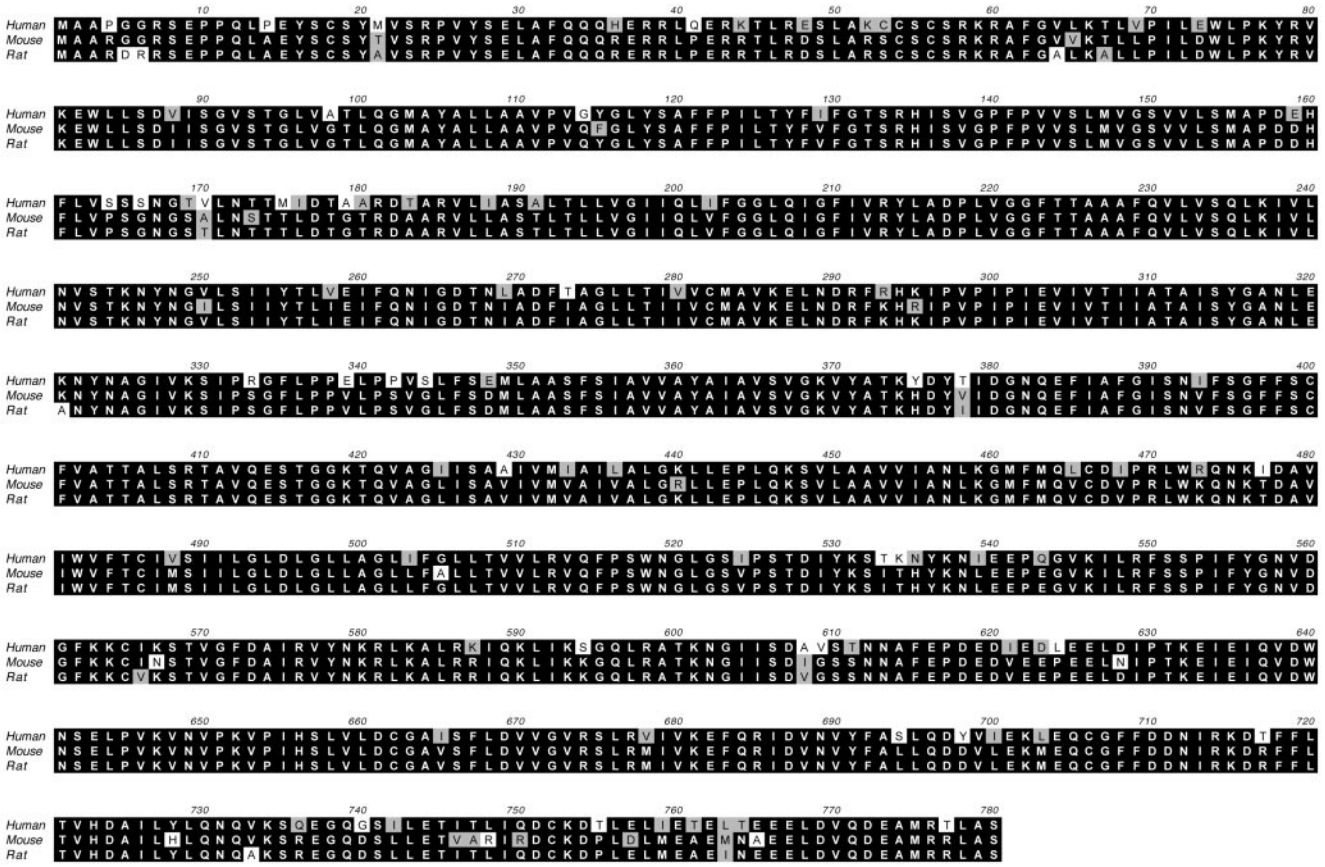

FIG. 1. Protein alignment of human, mouse, and rat pendrin. The amino acid sequences of pendrin from the indicated species are aligned relative to one another, as predicted from the cDNA sequences of human, mouse, and rat *PDS*/*Pds*. Amino acid residues that are identical among the three species are shown on a black background, whereas conservative substitutions are shaded in gray.

studies, especially in the developing inner ear. Previously, we detected *PDS* expression in a fetal cochlear cDNA library by using PCR analysis (12); however, these results did not provide any insight about the temporal or spatial pattern of *PDS* expression, which is important in light of the complexities of inner ear development and function. Thus, we performed RNA *in situ* hybridization of inner ear sections derived from mice at various developmental stages by using a *Pds*-derived riboprobe. As a guide to the results described below, Fig. 2*A* provides an anatomical overview of the fully developed mammalian inner ear.

At mouse postnatal day (P) 5, inner ear development is almost complete, and *Pds* is expressed in several discrete areas. The most pronounced *Pds* expression is seen in the endolymphatic duct and sac (Fig. 2*B*), with significant expression detected throughout both structures. Additional areas of *Pds* expression include the nonsensory regions of the utricle, saccule, and cochlea. In the utricle, *Pds* is expressed in a nonsensory region located between the macula utriculi (the sensory area of the utricle) and the cristae of the anterior and lateral semicircular canals (Fig. 2*C*). Likewise, in the saccule, *Pds* is expressed in a nonsensory region at the posterior tip of the medial wall close to the cochleosaccular duct (Fig. 2*D*), again adjacent to the macula. Note that P5 was the latest stage tested for *Pds* expression in the inner ear.

In the cochlea of a P5 mouse, *Pds* expression occurs within a restricted set of cells (see Fig. 3*A* for an overview of the relevant anatomy). Specifically, *Pds* is expressed by cells that reside immediately beneath the spiral prominence, on the lateral wall of the external sulcus (Fig. 3 *B* and *C*). To establish the cochlear expression pattern of *Pds* in a more precise fashion, parallel studies were performed with two genes known to be expressed in neighboring areas: *Tyrp2* (Fig. 3 *D* and *E*), which serves as a marker for melanocytes in the stria vascularis (20), and *Bmp4* (Fig. 3 *F* and *G*), which serves as a marker for Hensen's/Claudius' cells (19, 22). The results of these studies demonstrate that *Pds* is expressed by a set of cochlear cells that reside in a small, delimited area between *Tyrp2*- and *Bmp4*-expressing cells. Interestingly, a small zone of cells that express none of these three genes appears to be present on either side of the *Pds*-expressing cells (see Fig. 3*A* for a summary of these studies).

To establish the temporal pattern of *Pds* expression during development, RNA *in situ* hybridization was also performed on mouse embryos from 8 dpc to birth. Fig. 4*A* shows a photograph of a paint-filled endolymphatic space at 15 dpc, which highlights the anatomy of the membranous labyrinth. *Pds* expression is not detected in the mouse inner ear before 13 dpc. At 13 dpc, *Pds* is expressed in the developing endolymphatic duct and sac (Fig. 4*B*); this appears to be the only site of expression at this stage. At 15 dpc, *Pds* expression is also detected in the utricle and saccule (Fig. 4 *C* and *D*, respectively) in the same regions as in the more developed inner ear (e.g., Fig. 2 *C* and *D*). *Pds* expression in the cochlea itself also begins at 15 dpc, appearing in the posterolateral region of the descending proximal portion of the cochlea (see "1" in Fig. 4*E*) and into the greater curvature of the coiling distal portion (see "2" in Fig. 4*E*). To refine the anatomical location of *Pds* expression at these embryonic stages, parallel studies were again performed with a probe specific for *Bmp4*, which is expressed in the cochlea anlage as early as 11.5 dpc. From 12 dpc onwards, *Bmp4* expression is detected in the nonsensory region adjacent to the developing sensory hair cell area of the organ of Corti (19). The regions of *Pds* expression in both the proximal and distal portions of the cochlea overlap with that of *Bmp4* at 15 dpc (compare Fig. 4 *F* and *G*) but are distinct by 18 dpc (data not shown).

DISCUSSION

After our identification of *PDS* as the gene mutated in Pendred's syndrome (12), we pursued various avenues of investigation aiming to characterize the gene and its associated mutations (9, 10, 13, 14, 16) as well as to elucidate the function of its encoded protein, pendrin. These efforts should help to define the physiological role of this anion transporter and to

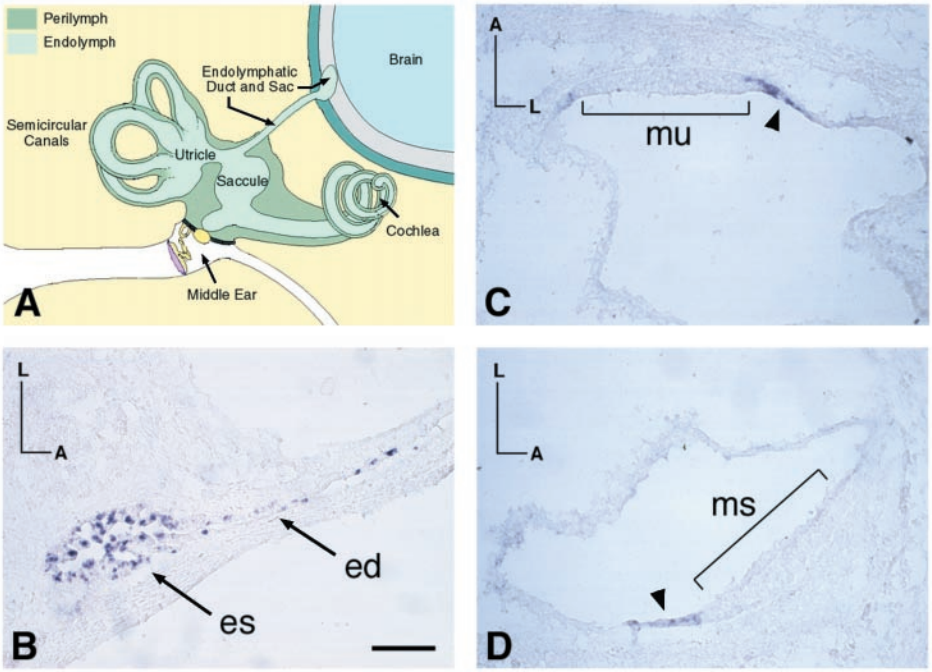

FIG. 2. RNA *in situ* hybridization of *Pds* in noncochlear regions of the mouse inner ear. (*A*) Anatomy of the fully developed mammalian inner ear (adapted from ref. 46). (*B–D*) Transverse sections (12 μm) through the inner ear of a P5 mouse were obtained and hybridized with a *Pds*-specific riboprobe. Note the detection of *Pds* expression (indicated by arrowheads) throughout the endolymphatic duct and sac (*B*) and in nonsensory regions of the utricle (*C*) and saccule (*D*), adjacent to the maculae in both of the latter cases. es, endolymphatic sac; ed, endolymphatic duct; mu, macula utriculi; ms, macula sacculi. Orientations: A, anterior; L, lateral. (Bar = 100 μm.)

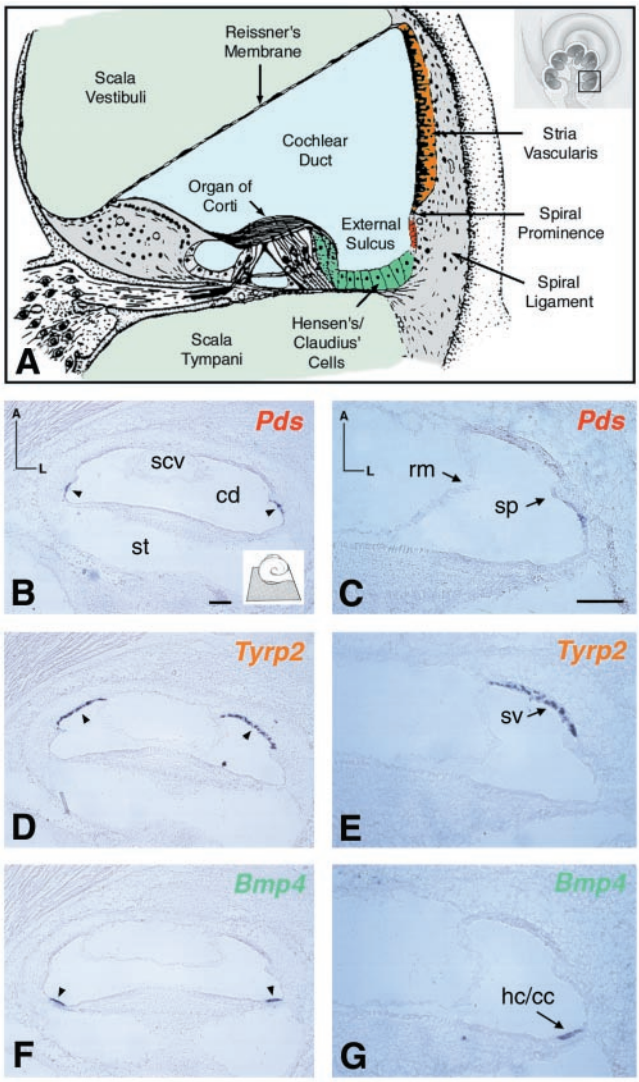

FIG. 3. RNA *in situ* hybridization of *Pds* in the mouse cochlea. (*A*) Annotated diagram showing a cross-section through one turn of the cochlea (adapted from http://www.bcm.tmc.edu/oto/studs/guineacochlea.gif; the *Inset* provides a global view of the diagram). (*B–G*) Transverse sections (12 μm) through the first turn of the cochlea of a P5 mouse were obtained and hybridized with *Pds*- (*B* and *C*), *Tyrp2*- (*D* and *E*), or *Bmp4*- (*F* and *G*) specific riboprobes. *B*, *D*, and *F* depict adjacent transverse sections, with analogous sections at higher magnifications shown in *C*, *E*, and *G*, respectively. The *Inset* in *B* roughly illustrates the manner in which the cochlea was sectioned for *B*, *D*, and *F* (provided to help illustrate why the lateral wall is seen on both sides of the cochlear duct). Note the detection of *Pds* expression in the lateral wall of the external sulcus within cells that reside between the regions of *Bmp4* and *Tyrp2* expression, respectively (compare *D* and *F* with *B* as well as *E* and *G* with *C*; expression indicated by arrowheads). There appear to be areas between *Pds*- and *Bmp4*-expressing cells as well as between *Pds*- and *Tyrp2*-expressing cells that do not show expression of any of these genes. *A* also provides a summary of these results, with orange reflecting the *Tyrp2*-expressing stria vascularis, green the *Bmp4*-expressing Hensen's/Claudius' cells, and red the *Pds*-expressing cells. scv, scala vestibuli; cd, cochlear duct (scala media); st, scala tympani; rm, Reissner's membrane; sp, spiral prominence; sv, stria vascularis; hc/cc, Hensen's/Claudius' cells. Orientations: A, anterior; L, lateral. (Bar = 100 μm.)

provide insight about the mechanism(s) underlying the deafness and goiter in Pendred's syndrome. Gaining a detailed understanding of pendrin's function in the inner ear will be especially challenging and realistically requires the use of a robust model system, such as the mouse. Motivated by the latter notion, we embarked on the studies reported here, which include elucidating the cDNA sequence of the mouse ortholog of the Pendred's syndrome gene (*Pds*) and characterizing the expression pattern of *Pds* in the developing inner ear.

Our studies of *Pds* expression shed new light on the role of pendrin during inner ear development and the etiology of deafness in Pendred's syndrome. Specifically, *Pds* is expressed in a limited set of cell types within the ear (Figs. 2–4). Furthermore, it is presumed that pendrin functions as an anion transporter within these cells. We postulate that the anion transport performed by pendrin is critical for maintaining the appropriate ionic balance within inner ear fluid, which is known to serve a crucial role in the hearing process (for review, see refs. 23–25). The inner ear consists of an inner and outer chamber (Fig. 2*A*). The outer chamber is encased by the bony labyrinth and contains a fluid called perilymph, which is similar in composition to cerebrospinal fluid. The inner chamber is separated from the outer chamber by a delicate membrane, the membranous labyrinth, and contains endolymph. Endolymph has a markedly different ionic composition from plasma and extracellular fluid (for review, see ref. 23). Indeed, its high potassium and very low sodium content more closely resembles intracellular fluid. Furthermore, endolymph has a positive voltage (+80 mV) compared with perilymph or plasma; this is called the endocochlear potential. The mechanisms required for the maintenance of this unusual fluid composition are poorly understood at present, but are appreciated to be complex and different from those of other fluid compartments.

The expression pattern of *Pds* may provide important clues about the possible role for pendrin in maintaining the appropriate ionic composition of inner ear fluid. In the cochlear duct, endolymph is mainly secreted by the marginal cells of the stria vascularis, the richly vascularized epithelium in the lateral wall (Fig. 3*A*); it is also believed to be secreted by other specialized cells of the inner ear, including the dark cells of the vestibule. However, the resorption of endolymph is thought to occur in the endolymphatic duct and sac, which, importantly, is the primary area of *Pds* expression. The endolymphatic duct and sac are extensions of the endolymphatic space, protruding through the vestibular aqueduct of the petrous temporal bone to the cranial cavity (Fig. 2*A*). Experimental destruction of the endolymphatic sac [e.g., for creating an animal model of Ménière's disease (26–29)] leads to an increased volume of endolymph with distension of the membranous labyrinth (endolymphatic hydrops), suggesting that the endolymphatic duct and sac play an important role in endolymph resorption. This is further supported by the fact that the characteristics of the cells in these structures are similar to those of other known ion- and fluid-transporting cells (30).

The endolymphatic duct and sac are widely studied for their role in the resorption of endolymph. It is interesting to note that some studies have indicated that the other *Pds*-expressing regions may also be involved in fluid homeostasis. Relatively little is known about the cells in the lateral wall of the external sulcus of the cochlear duct, and *Pds* is the first gene associated with expression specific to these cells. To date, there have been two cell types described in this region, most easily distinguishable at an electron microscopy level. The spiral prominence cells extend down from the stria vascularis to meet the external sulcus root cells, which in turn are almost totally covered by the Claudius' cells (31). Based on our light microscopy studies, we cannot establish precisely which of the two cell types in the external sulcus expresses *Pds*. This is further complicated by the fact that at P5 (the latest stage examined), the mouse cochlea is not fully developed (32). Indeed, given that *Pds* expression is not directly adjacent to the stria vascularis or the Claudius' cells, it would appear that there could be more than two cell types in this region at a functional level. However, there is evidence suggesting that both the spiral prominence

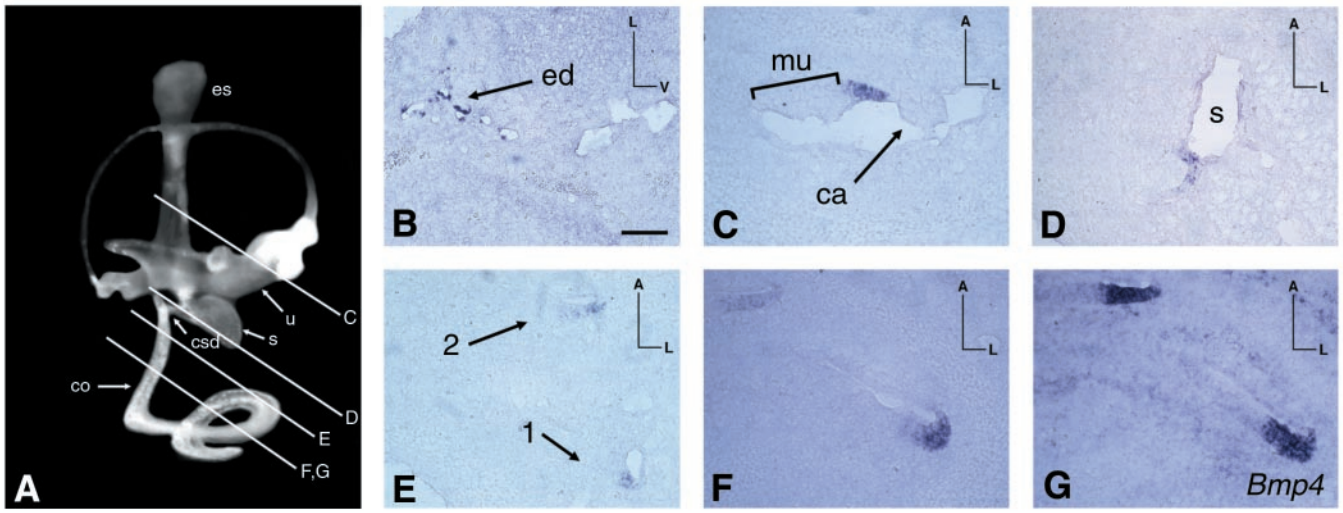

FIG. 4. RNA *in situ* hybridization of *Pds* in the developing mouse inner ear. (*A*) Photograph of a paint-filled endolymphatic space of a developing mouse inner ear at 15 dpc showing the planes of the sections depicted in *C–G*. A coronal 12-μm section from a 13-dpc mouse inner ear (*B*) or transverse 12-μm sections from 15-dpc mouse inner ears (*C–G*) were obtained and hybridized with *Pds*- (*B–F*) or *Bmp4*- (*G*) specific riboprobes. *F* and *G* depict adjacent sections. At 13 dpc, *Pds* expression is detected in the endolymphatic duct and sac (*B*). At 15 dpc, *Pds* expression is found in the utricle (*C*), saccule (*D*), and cochlea (*E* and *F*). Note that at 15 dpc, the *Pds*- and *Bmp4*-expressing areas overlap (compare *F* and *G*). es, endolymphatic sac; u, utricle; s, saccule; csd, cochleosaccular duct; co, cochlea; ed, endolymphatic duct; mu, macula utriculi; ca, crista ampullaris; s, saccule; 1, proximal portion of the cochlea; 2, distal portion of the cochlea. Orientations: L, lateral; V, ventral; A, anterior. (Bar = 100 μm.)

cells (33–35) and the external sulcus root cells (31, 36, 37) play a role in fluid resorption (and possibly secretion). In the utricle and saccule, *Pds* expression is seen adjacent to the maculae, and thus the *Pds*-expressing cells here probably represent the transitional cells (or a subset of them). The presence of Na^+/K^+-ATPase specifically in these cells (38), but not neighboring cells, also suggests a role in the homeostasis of inner ear fluids. Finally, it is interesting to note that all of the *Pds*-expressing cells in the inner ear also express the gene encoding AE2 (39), a Cl^-/HCO_3^- exchanger, although the latter has a slightly wider expression pattern (40).

Taken together, our data indicate that *Pds* is expressed in several different types of inner ear cells that are important for the resorption of endolymph. These results are particularly interesting in light of the recent report of Scott *et al.* (17) demonstrating that pendrin functions to transport iodide and chloride (but not sulfate). Iodide is not of known importance in the inner ear, whereas a role for chloride can be readily postulated. Additional studies are needed to identify which anion(s) are being transported by pendrin within the inner ear. Regardless, these findings allow hypotheses to be formulated about the pathology seen in Pendred's syndrome. At first, it seems difficult to imagine how altered fluid homeostasis can cause what is essentially an arrest in development of the inner ear at seven weeks of gestation (e.g., resulting in a Mondini malformation or widened vestibular aqueduct). However, assuming that pendrin function and *PDS*/*Pds* expression patterns are conserved between human and mouse inner ears, one can speculate that if resorption of fluid is inefficient at a critical developmental stage, the increased endolymphatic volume could cause an abnormal fluid pressure that hinders the final maturation of the inner ear and leads to this patterning defect. It is important to point out that a widespread endolymphatic hydrops has not been described in adults with Pendred's syndrome, even in the presence of an enlarged endolymphatic sac. This suggests that there is either a critical stage of inner ear development particularly sensitive to the putative resorption defect or a compensatory resorption mechanism that sets in after cochlear development.

Although the deafness in Pendred's syndrome is generally congenital, there are a smaller number of cases with later-onset hearing loss, often being precipitated by mild head trauma (7, 9, 10, 41). Of the above-referenced cases that were investigated radiologically, this late-onset presentation was usually associated with enlarged vestibular aqueducts. It is assumed that if the hearing loss is of later onset, the sensory and neural cells of the cochlea must have (at least initially) developed normally. However, it has been suggested that a large vestibular aqueduct allows the abnormal transmission of fluid pressure from the cranial cavity, which may cause a rupture of the membranous labyrinth in congenitally weak spots of the basilar membrane or Reissner's membrane. In turn, leakage of the potassium-rich neurotoxic endolymph could then damage the sensory and nerve cells, resulting in deafness (42). Of course, it is also possible that this is the etiology underlying the hearing loss in patients with congenital (or at least prelingual) deafness.

It is worth noting that our data on *Pds* expression strongly suggests that the deafness in Pendred's syndrome is directly caused by the absence of normal pendrin in the inner ear as opposed to a secondary effect of thyroid dysfunction. The latter notion has (at times) been speculated in light of the well known association of congenital hypothyroidism and deafness. Other arguments against such a theory include the fact that hypothyroidism-induced deafness in animal models generally affects the organ of Corti and tectorial membrane in a specific fashion (43, 44) and thus differs from the defects seen in Pendred's syndrome. Furthermore, overall thyroid function, as assessed by serum thyroid-stimulating hormone and thyroid hormone levels, is generally normal in Pendred's syndrome and, in the fetus, maternal hormones would compensate for any tendency toward a hypothyroid state. Finally, even with severe congenital hypothyroidism, hearing loss is often mild (45).

In the studies reported here, we have investigated the function of pendrin in the inner ear. However, analogous questions regarding the role of pendrin in the thyroid gland and in other *Pds*-expressing tissues are also of interest. For example, we have preliminary evidence for the presence of pendrin in a limited subset of thyroid follicular cells but not in C cells. Furthermore, the expression of *Pds* appears to be under complicated regulatory controls involving thyroglobulin (K. Suzuki, I. Royaux, L.A.E., L. D. Kohn, and E.D.G.,

unpublished data). These studies also point to distinct functions for pendrin in the thyroid and inner ear.

In summary, the results reported here represent important first steps toward defining the role of pendrin in the inner ear. In particular, our expression studies give tantalizing clues about the possible etiology of deafness in Pendred's syndrome centering on defective anion transport and endolymphatic fluid homeostasis. Future studies will be aided by the development of a *Pds*-knockout mouse, which should provide valuable information about the functioning of pendrin in the inner ear, the thyroid, and other tissues as well as an experimental system for investigating all of the clinical features of Pendred's syndrome.

We thank Drs. Jim Battey, Tom Friedman, and Andy Griffith for critical review of this manuscript. We also thank Brigid Hogan and Ian Jackson for providing probes.

1. Pendred, V. (1896) *Lancet* **II,** 532.
2. Reardon, W. & Trembath, R. C. (1996) *J. Med. Genet.* **33,** 1037–1040.
3. Reardon, W., Coffey, R. & Trembath, R. (1997) *Q. J. Med.* **90,** 443–447.
4. Johnsen, T., Sorensen, M. S., Feldt-Rasmussen, U. & Friis, J. (1989) *Clin. Otolaryngol.* **14,** 395–399.
5. Mondini, C. (1791) *Bononiae* **7,** 419–431.
6. Johnsen, T., Jorgensen, M. B. & Johnsen, S. (1986) *Acta Otolaryngol.* **102,** 239–247.
7. Johnsen, T., Larsen, C., Friis, J. & Hougaard-Jensen, F. (1987) *J. Laryngol. Otol.* **101,** 1187–1192.
8. Phelps, P. D., Coffey, R. A., Trembath, R. C., Luxon, L. M., Grossman, A. B., Britton, K. E., Kendall-Taylor, P., Graham, J. M., Cadge, B. C., Stephens, S. G., *et al.* (1998) *Clin. Radiol.* **53,** 268–273.
9. Cremers, W. R., Bolder, C., Admiraal, R. J., Everett, L. A., Joosten, F. B., Van Hauwe, P., Green, E. D. & Otten, B. J. (1998) *Arch. Otolaryngol. Head Neck Surg.* **124,** 501–505.
10. Cremers, C. W., Admiraal, R. J., Huygen, P. L., Bolder, C., Everett, L. A., Joosten, F. B., Green, E. D., Van Camp, G. & Otten, B. J. (1998) *Int. J. Pediatr. Otorhinolaryngol.* **45,** 113–123.
11. Schuknecht, H. F. (1980) *Ann. Otol. Rhinol. Laryngol. Suppl.* **89,** 1–23.
12. Everett, L. A., Glaser, B., Beck, J. C., Idol, J. R., Buchs, A., Heyman, M., Adawi, F., Hazani, E., Nassir, E., Baxevanis, A. D., *et al.* (1997) *Nat. Genet.* **17,** 411–422.
13. Li, X. C., Everett, L. A., Lalwani, A. K., Desmukh, D., Friedman, T. B., Green, E. D. & Wilcox, E. R. (1998) *Nat. Genet.* **18,** 215–217.
14. Van Hauwe, P., Everett, L. A., Coucke, P., Scott, D. A., Kraft, M. L., Ris-Stalpers, C., Bolder, C., Otten, B., de Vijlder, J. J. M., Dietrich, N. L., *et al.* (1998) *Hum. Mol. Genet.* **7,** 1099–1104.
15. Coyle, B., Reardon, W., Herbrick, J. A., Tsui, L. C., Gausden, E., Lee, J., Coffey, R., Grueters, A., Grossman, Phelps, P. D., *et al.* (1998) *Hum. Mol. Genet.* **7,** 1105–1112.
16. Coucke, P., Van Hauwe, P., Everett, L. A., Demirhan, O., Kabakkaya, Y., Dietrich, N. L., Smith, R. J. H., Coyle, E., Reardon, W., Trembath, R., *et al.* (1999) *J. Med. Genet.* **36,** 475–477.
17. Scott, D. A., Wang, R., Kreman, T. M., Sheffield, V. C. & Karniski, L. P. (1999) *Nat. Genet.* **21,** 440–443.
18. Theiler, K. (1989) *The House Mouse: Atlas of Embryonic Development* (Springer, New York).
19. Morsli, H., Choo, D., Ryan, A., Johnson, R. & Wu, D. K. (1998) *J. Neurosci.* **18,** 3327–3335.
20. Steel, K. P., Davidson, D. R. & Jackson, I. J. (1992) *Development (Cambridge, U.K.)* **115,** 1111–1119.
21. Frohman, M. A., Dush, M. K. & Martin, G. R. (1988) *Proc. Natl. Acad. Sci. USA* **85,** 8998–9002.
22. Takemura, T., Sakagami, M., Takebayashi, K., Umemoto, M., Nakase, T., Takaoka, K., Kubo, T., Kitamura, Y. & Nomura, S. (1996) *Hear. Res.* **95,** 26–32.
23. Sterkers, O., Ferrary, E. & Amiel, C. (1988) *Physiol. Rev.* **68,** 1083–1128.
24. Ferrary, E. & Sterkers, O. (1998) *Kidney Int. Suppl.* **65,** S98–103.
25. Fritzsch, B. & Beisel, K. (1998) *Am. J. Hum. Genet.* **63,** 1263–1270.
26. Kimura, R. S. (1967) *Ann. Otol. Rhinol. Laryngol.* **76,** 664–687.
27. Kerr, A. G. & Smyth, G. D. (1976) *J. Laryngol. Otol.* **90,** 841–843.
28. Kimura, R. S. (1982) *Am. J. Otolaryngol.* **3,** 447–451.
29. Merchant, S. N., Rauch, SD & Nadol, J. B. J. (1995) *Eur. Arch. Otorhinolaryngol.* **252,** 63–75.
30. Lundquist, P. G., Rask-Andersen, H., Galey, F. R. & Bagger-Sjöbäck, D. (1984) in *Ultrastructural Morphology of the Endolymphatic Duct and Sac,* eds. Friedmann, I. & Ballantyne, J. (Butterworth, London), pp. 309–325.
31. Kucuk, B. & Abe, K. (1990) *Arch. Histol. Cytol.* **53,** 297–305.
32. Lim, D. J. & Anniko, M. (1985) *Acta Otolaryngol. Suppl. (Stockh.)* **422,** 1–69.
33. Mees, K. (1982) *Laryngol. Rhinol. Otol. (Stuttg.)* **61,** 595–600.
34. Mees, K. (1982) *Arch. Otorhinolaryngol.* **236,** 41–51.
35. Mees, K. (1983) *Laryngol. Rhinol. Otol. (Stuttg.)* **62,** 597–602.
36. Kimura, R. S. & Ota, C. Y. (1974) *Acta Otolaryngol.* **77,** 231–250.
37. Hawkins, J. E. J. (1976) *Arch. Otorhinolaryngol.* **212,** 241–251.
38. Spicer, S. S., Schulte, B. A. & Adams, J. C. (1990) *Hear. Res.* **43,** 205–217.
39. Gehrig, H., Muller, W. & Appelhans, H. (1992) *Biochim. Biophys. Acta* **1130,** 326–328.
40. Stankovic, K. M., Brown, D., Alper, S. L. & Adams, J. C. (1997) *Hear. Res.* **114,** 21–34.
41. Das, V. K. (1987) *J. Laryngol. Otol.* **101,** 721–722.
42. Jackler, R. K. & De La Cruz, A. (1989) *Laryngoscope* **99,** 1238–1242.
43. Uziel, A., Gabrion, J., Ohresser, M. & Legrand, C. (1981) *Acta Otolaryngol.* **92,** 469–480.
44. O'Malley, B. W., Jr., Li, D. & Turner, D. S. (1995) *Hear. Res.* **88,** 181–189.
45. Debruyne, F., Vanderschueren-Lodeweyckx, M. & Bastijns, P. (1983) *Audiology* **22,** 404–409.
46. Kalatzis, V. & Petit, C. (1998) *Hum. Mol. Genet.* **7,** 1589–1597.